Aldehyde Dehydrogenase Activity of *Drosophila melanogaster* Alcohol Dehydrogenase: Burst Kinetics at High pH and Aldehyde Dismutase Activity at Physiological pH†

Gary T. M. Henehan,‡ Simon H. Chang,§ and Norman J. Oppenheimer*,‡

Department of Pharmaceutical Chemistry S-926, University of California, San Francisco, San Francisco, California 94143-0446, and Department of Biochemistry and Zoology, Louisiana State University, Baton Rouge, Louisiana 70803

Received April 17, 1995; Revised Manuscript Received June 30, 1995⊗

ABSTRACT: The ability of *Drosophila* alcohol dehydrogenase (D-ADH) to catalyze the oxidation of aldehydes to carboxylic acids has been re-examined. Prior studies are shown to have been compromised by a nonenzymic reaction between the aldehydic substrates and amine-containing buffers, e.g., glycine or Tris, and an amine-catalyzed addition of aldehyde to NAD^+. These reactions interfere with spectrophotometric assays for monitoring aldehyde oxidation and obscure the nature and scope of D-ADH-catalyzed aldehyde oxidation, particularly at physiological pH. Use of nonreactive buffers, such as pyrophosphate or phosphate, and ^1H NMR spectroscopy to monitor all the components of the reaction mixture reveals the facile dismutation of aldehydes into equimolar quantities of the corresponding acids and alcohols at both neutral and high pH. At high pH, dismutation is accompanied by a small burst of NADH production to a steady-state concentration (<10 μM) that represents a partitioning between NADH dissociation and aldehyde reduction. The increase in A_{340} is therefore not a direct measure of the aldehyde oxidation reaction, and the resulting kinetic values cannot be compared to those for alcohol dehydrogenation. The present results for D-ADH, combined with data from the literature, establish that aldehyde oxidation, manifest as dismutation, is a widespread property of alcohol dehydrogenases with potential physiological importance in alcohol metabolism and aldehyde detoxification.

Recent studies in this laboratory have focused on the largely unrecognized ability of horse liver alcohol dehydrogenase (HL-ADH)[1] to oxidize aldehydes to carboxylic acids (Henehan et al., 1993; Henehan & Oppenheimer, 1993; Oppenheimer & Henehan, 1995). Because of the reported high K_m (Dalziel & Dickinson, 1965) and low V_{max} (Hinson & Neal, 1972) for aldehyde oxidation, this activity (reaction 1) had been considered to be an insignificant side reaction of the "normal" alcohol dehydrogenation activity shown in reaction 2, where R is an H, alkyl, or aryl group.

$$RCHO + NAD^+ \rightarrow RCOOH + NADH + H^+ \quad (1)$$

$$RR'CHOH + NAD^+ \rightleftharpoons RR'CO + NADH + H^+ \quad (2)$$

This view was further reinforced by the fact that yeast alcohol dehydrogenase, which is structurally similar and mechanistically identical to HL-ADH (Jörnvall et al., 1978), reportedly does *not* exhibit this activity (Dickinson & Monger, 1973). Indeed, HL-ADH is the only *alcohol* dehydrogenase that displays aldehyde dehydrogenase activity at physiological pH, i.e., generation of NADH when incubated with NAD^+ and aldehyde (Hinson & Neal, 1972; Tsai & Sher, 1980; Henehan et al., 1993; Henehan & Oppenheimer, 1993; Oppenheimer & Henehan, 1995). Our recent studies have shown, however, that the activity of HL-ADH is kinetically more complex than previously thought (Henehan & Oppenheimer, 1993) and involves the rapid dismutation of the aldehyde substrate (reaction 3) prior to any production of NADH.

$$2RCHO \rightarrow ROH + RCOOH \quad (3)$$

Drosophila alcohol dehydrogenase (D-ADH) has also been reported to catalyze the oxidation of aldehydes to carboxylic acids. This conclusion was based on spectrophotometric measurements made of an enzyme-dependent increase in A_{340} at elevated pH (≥9.5) attributed to the generation of NADH (Heinstra et al., 1983; Moxon et al., 1985; Eisses, 1989). Furthermore, unlike the reportedly poor catalytic efficiency of HL-ADH, the rates of acetaldehyde oxidation catalyzed by D-ADH were comparable to those of ethanol oxidation (Moxon et al., 1985); however, this reaction was only observed at high pH. At neutral pH no increase in A_{340} was observed. These results lead to the conclusion that the aldehyde oxidation activity of D-ADH was unlikely to be physiologically relevant because of its high pH optimum (Benner et al., 1985; Brooks et al., 1985). In conflict with

† This research was supported in part by National Institutes of Health Grant GM-22982, GM-52529 (N.J.O.), and ES-03347 (S.H.C.). The UCSF Magnetic Resonance Laboratory is in part funded by grants from the National Science Foundation (DMB-8406826) and the National Institutes of Health (RR-01668).

* Corresponding author. Phone: (415) 476-3038 (office), (415) 476-0688 (fax); E-Mail: oppen@cgl.ucsf.edu.

‡ University of California, San Francisco.

§ Louisiana State University, Baton Rouge.

⊗ Abstract published in *Advance ACS Abstracts,* September 1, 1995.

[1] Abbreviations: D-ADH, *Drosophila* alcohol dehydrogenase; HL-ADH, horse liver alcohol dehydrogenase; CAPS, 3-(cyclohexylamino)-1-propanesulfonic acid; ^1H NMR, proton nuclear magnetic resonance; A_{340}, absorbance at 340 nm; λ_{max}, wavelength of maximum absorption; Tris, tris(hydroxymethyl)aminomethane; NAD^+, nicotinamide adenine dinucleotide (oxidized form); NADH, nicotinamide adenine dinucleotide (reduced form); E, enzyme; ADH, alcohol dehydrogenase; pD = pH meter reading + 0.4 (Glasoe & Long, 1960).

0006-2960/95/0434-12294$09.00/0

these *in vitro* observations are *in vivo* studies that indicated the participation of this second catalytic activity of D-ADH in the metabolism of ethanol-derived acetaldehyde (Heinstra et al., 1989). Further inconsistencies are evident in the kinetic properties of the enzyme-catalyzed aldehyde oxidation at high pH; some workers report Michaelis−Menten kinetics (Eisses, 1989) while others report significant deviation from hyperbolic behavior (Moxon et al., 1985).

In order to explore the generality of the property of alcohol dehydrogenases to oxidize aldehydes, we have begun an investigation of the ability of D-ADH to conduct aldehyde oxidation. D-ADH was chosen because it is a member of an evolutionarily distinct family of alcohol dehydrogenases from that represented by HL-ADH. The "short" alcohol dehydrogenases are ca. 10 kDa smaller per subunit than "medium" alcohol dehydrogenases, they do not contain a catalytic metal atom, and they conduct hydride transfer with *pro-S* stereochemistry versus the *pro-R* specificity of the "medium" ADHs (for a discussion, see Persson et al., 1991).

In this paper we demonstrate that the previously reported properties of the aldehyde oxidation catalyzed by D-ADH have been compromised by a combination of artifacts arising from reaction of the aldehyde substrate with the widely-used amine buffers, catalysis of NAD−aldehyde adduct formation by these buffers, and the reliance on changes in A_{340} as the sole determinant of reaction progress. When these artifacts are taken into account, we find that D-ADH catalyzes a rapid aldehyde dismutation at physiological pH and that the increase in A_{340} observed at high pH represents a burst to <10 μM NADH and is not a direct measure of the rate of aldehyde oxidation.

EXPERIMENTAL PROCEDURES

Materials. NAD^+ was obtained from the Sigma Chemical Co. and used without further purification. Other chemicals, buffers, and substrates were obtained from Aldrich and were of the highest purity available. Acetaldehyde was distilled under a stream of oxygen-free nitrogen, diluted 1:10 with double-distilled deionized water, and stored frozen in aliquots at −20 °C until used. NAD^+ concentrations were determined spectrophotometrically (ϵ_{260} = 18 000 mol^{-1} cm^{-1}).

Enzyme Preparation and Assay. Construction of the recombinant wild-type D-ADH as well as purification of the expressed protein is described by Chen et al. (1990). Spectrophotometric measurements were performed on a Hewlett-Packard 8542A diode-array spectrophotometer thermostated at 30 °C. The time-dependent increase in A_{340} was measured in stoppered cuvettes under conditions noted in the appropriate figure legends. Enzyme stock solutions were prepared in 5 mM sodium phosphate buffer, pH 7.5. The specific activity of D-ADH preparations was determined by assay in 0.1 M phosphate buffer, pH 7.5, in the presence of saturating substrate concentrations, 2.0 mM NAD^+, and 88 mM ethanol (Moxon et al., 1985).

^1H NMR Spectroscopy. Proton nuclear magnetic spectra were acquired at 500 MHz on a General Electric GN-500 instrument. The probe temperature was maintained at 30 °C, and 5 mm NMR tubes were used. The final NMR sample volume was 0.5 mL. For kinetic runs, spectra were acquired every 8.15 min and consisted of 64 scans with a spectral width of 6000 Hz, using 16K data points. The reactions were conducted in aqueous buffers, with 10% D_2O added to provide a lock signal. Suppression of the water resonance was achieved using solvent presaturation with a decoupler pulse (Hore, 1989). The observe pulse width was set to correspond to a 45° tip angle, and a 6.0 s presaturation pulse was used. These conditions assured equilibrium intensities for resonances more than 1 ppm from the water peak. The concentration of enzyme was adjusted to optimize the rate of the enzyme-catalyzed reaction to the time resolution of spectral acquisition. The integrated area of the resonances for each component was measured and their concentration calculated relative to the integrated areas of the nicotinamide ring protons of NAD^+. Coenzyme concentration was determined spectrophotometrically before and after each run and found to remain unchanged. The reported aldehyde concentrations represent the sum of free and hydrated species present in a 1:0.83 ratio, respectively, at 30 °C and pH 7.5.

For the NMR assay of the dismutation reaction, NAD^+, acetaldehyde, and buffer were preincubated for 10 min to allow temperature equilibration before a control spectrum was taken. Enzyme was then added to the NMR tube to initiate the reaction, giving a final volume of 500 μL. Acetaldehyde consumption was measured by following the disappearance of the methyl group of the free aldehyde form which gives rise to a 3H doublet at 2.23 ppm. The resonance of the aldehydic proton, a ^1H quartet at 9.67 ppm, and the hydrate methyl proton, a 3H doublet at 1.32 ppm, were also measured. Acetate formation was monitored by following the appearance of its methyl group, which gave rise to a sharp, 3H singlet at 1.90 ppm. Ethanol formation was followed by monitoring the appearance of its methyl group, a 3H triplet at 1.17 ppm.

RESULTS

Reproduction of the "Standard" Assay for Aldehyde Oxidation by Drosophila Alcohol Dehydrogenase. Previous studies of the "aldehyde dehydrogenase" activity of D-ADH (Heinstra et al., 1983; Moxon et al., 1985) were thought to measure the direct oxidation of an aldehyde to a carboxylic acid by monitoring the increase in A_{340} of the concomitant reduction of NAD^+ to NADH (see reaction 1). This approach was considered appropriate because aldehyde oxidation is irreversible, hence NADH production was assumed to be a direct measure of aldehyde oxidation.

We have reproduced standard assays conducted at 30 °C in Tris or glycine buffer, pH 9.5−10, containing 1−2 mM NAD^+ and a range of 0.1−20 mM acetaldehyde and can obtain kinetic values to within 20% those reported in the literature (Heinstra et al., 1983; Moxon et al., 1985; Eisses, 1989). Like the previous studies, we find that high pH is necessary for the assay because no increase in A_{340} is observed at neutral pH (Benner et al., 1985; Brooks et al., 1985). As we will develop, however, data obtained with these assays and the kinetic values derived therefrom are misleading and cannot be used to assess the true kinetic properties of aldehyde oxidation by D-ADH.

$$RCHO + R'NH_2 \rightleftharpoons RCH(OH)NHR' \rightleftharpoons RCH{=}NR' \rightarrow \text{polymers} \quad (4)$$

Reactions of Aldehydes with Primary Amines. A central problem in the previous assays of aldehyde oxidation by D-ADH is the use of buffers that react with the aldehyde

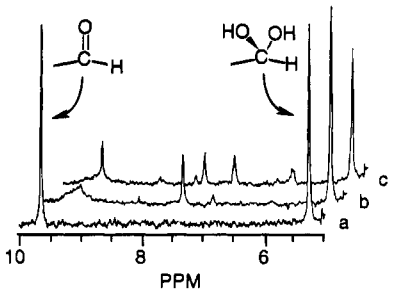

FIGURE 1: The downfield region of the 500 MHz ^{1}H NMR spectrum showing the aldehydic proton resonance of 10.0 mM acetaldehyde at 30 °C. Spectrum a: 0.1 M pyrophosphate, pD 9.5. Spectrum b: 0.1 M glycine buffer, pD 9.5, immediately after adding acetaldehyde. Spectrum c: the same sample as (b) 1 h after addition of acetaldehyde. The sample in pyrophosphate buffer showed no detectable change after one hour (not shown).

substrates. Many common buffers, such as Tris, glycine, or bicine, contain primary amines. Aliphatic aldehydes, and other aldehydes containing strongly electron-withdrawing substituents, rapidly react with the unprotonated form of amino groups to give carbinolamines, which dehydrate to Schiff bases, and then subsequently polymerize to higher molecular weight products (reaction 4). The fate of acetaldehyde in glycine buffer at high pH under the standard assay conditions for aldehyde oxidation can be readily followed by NMR. In Figure 1, the downfield portion of the ^{1}H NMR spectrum of 10 mM acetaldehyde in sodium pyrophosphate buffer, pD 9.5, 30 °C, is compared to the corresponding spectral region for 10 mM acetaldehyde in 100 mM glycine buffer at pD 9.5. Acetaldehyde in pyrophosphate shows the expected resonances for both the free aldehyde and hydrated forms. Immediately upon addition of acetaldehyde to the glycine buffer, the aldehydic resonance at 9.67 ppm becomes severely broadened (linewidth > 100 Hz) and shifts slightly upfield. A new resonance also appears upon mixing at 7.70 ppm, which we attribute to the Schiff base, and represents about 10% of the initial acetaldehyde. There is no obvious effect on the acetaldehyde hydrate resonance at 5.23 ppm. With time, a new, sharp aldehydic peak appears at 9.37 ppm, 0.3 ppm upfield from the initial chemical shift of acetaldehyde. In 1 h under these conditions, this resonance increases until it represents ca. 8% of the total initial acetaldehyde. The appearance of other new resonances is also noted at 7.8 and 7.2 ppm in the olefinic region. During this time the resonances of the original Schiff base decrease markedly along with a concomitant decrease in the resonances of the hydrate. In all, after an hour incubation at 30 °C approximately 35% of the initial acetaldehyde has been converted to various products. A similar sequence of reactions is observed for Tris buffer (not shown). When acetaldehyde is dissolved in pyrophosphate buffer and incubated under the same conditions, no detectable changes in the ^{1}H NMR spectrum are observed.

These results are consistent with an initial reaction and equilibration of the free aldehyde and amine buffer to yield a carbinolamine and Schiff base (reaction 4). The absence of any kinetic broadening of the resonances of the Schiff base establishes that the carbinolamine is in slow exchange with the Schiff base. The maintenance of a constant ratio of Schiff base to the aldehyde hydrate indicates that the Schiff base, carbinolamine, aldehyde hydrate, and free aldehyde are all in equilibrium on the time scale of the measurement, but

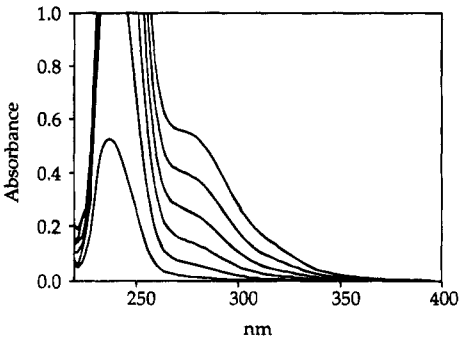

FIGURE 2: Time-dependent change in the UV spectrum of 1 mM acetaldehyde incubated in 0.1 mM glycine buffer at pH 9.5 and 30 °C with a 10 min interval between spectra.

in slow exchange with respect to the individual resonances in the NMR spectrum. As can be seen in Figure 1, a multiplicity of uncharacterized polymerization products (reaction 4) appear within an hour, and their concentrations increase with a concomitant decrease in the original resonances. Of special note is the new aldehydic proton that arises at 9.37 ppm. It remains narrow and sharp, indicating the absence of any exchange broadening from reaction with glycine. This observation suggests that the new aldehyde group is in conjugation with a double bond, thereby much less likely to form a carbinolamine. The presence of a conjugated aldehyde is also consistent with the appearance of new resonances in the spectral region from 8 to 6 ppm where olefinic protons are normally found, and in the changes observed for the UV absorption spectrum.

Incubation of acetaldehyde at one-tenth the concentration used for ^{1}H NMR spectroscopy yields a new absorption in the UV spectrum, initially centered at 230 nm (see Figure 2). This absorption rapidly increases and broadens in the direction of higher wavelengths. A distinct shoulder also develops at 280 nm, and with time, a hint of a second shoulder appears at longer wavelengths, as can be seen in Figure 2. Within an hour the solution develops a reddish-brown color due to this formation of chromophores at increasingly longer wavelengths, which causes a general increase in absorbance out to almost 600 nm. This result is consistent with the formation of a variety of secondary polymerization products containing conjugated olefins and carbonyls. Obviously, the detailed characterization of the myriad of reaction products is beyond the scope of this investigation, Clearly, however, glycine and other primary amine-containing buffers are unsuitable for the assay of enzymes utilizing aldehydes as substrates. The important point is that aldehydes remain unaffected in nonreactive buffers such as pyrophosphate or CAPS.

Blank Rates in the Spectrophotometric Assay. As described above, a pronounced nonenzymic blank reaction is observed when the standard assay conditions are used to monitor the reaction at 340 nm. In the experiments presented below, this blank reaction was found to consist of two components. The first component (blank I) results from the reaction between the aldehyde substrate and glycine or Tris buffer, giving rise to a general increase in absorption from 200 to 600 nm as discussed above. A second component (blank II) is a specific increase in absorbance with a λ_{max} at 340 nm that occurs when NAD^+ is added to an aldehyde solution in glycine or Tris buffers at high pH.

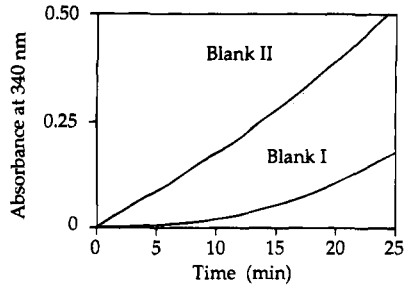

FIGURE 3: Progress curves showing the two components of the blank reaction observed at 340 nm for the spectrophotometric assay of aldehyde oxidation by D-ADH. Blank I results from the addition of acetaldehyde at a final concentration of 20 mM to a 0.1 M glycine buffer, pH 9.5. Blank II results from the addition of acetaldehyde at a final concentration of 20 mM to a 0.1 M glycine buffer, pH 9.5, containing 2.0 mM NAD^+.

Blank I. A key aspect of the blank I reaction for incubation of acetaldehyde in a solution of 0.1 M glycine buffer, pH 9.5, is the pronounced lag in A_{340} that occurs (see Figure 3). Because of this nonlinear property, the blank I reaction can go unobserved at 340 nm when assays are started by addition of aldehyde and the progress curves are followed for only a short period of time; e.g., typical conditions employed for initial rate measurements. The impact of the blank I reaction becomes increasingly significant in the following situations: (i) where assays are carried out over a longer period of time, (ii) when the aldehyde substrate is preincubated in the assay mixture before initiating the reaction by enzyme addition, or (iii) if concentrated stock solutions of aldehyde are made up in the assay buffer prior to use. Any of these conditions singly or in combination can result in seriously compromised data. Nowhere will this blank reaction be more important than when the nonenzymatic increase in A_{340}, based on observing the first few minutes of an incubation prior to adding enzyme, is *linearly* extrapolated to serve as a measure of the blank reaction for the duration of a much longer assay incubation.

Blank II. A second component of the blank reaction, blank II, occurs when NAD^+ is added to the assay mixture. As shown in Figure 3, addition of 2.0 mM NAD^+ to 20 mM acetaldehyde in 0.1 M glycine, pH 9.5, causes an immediate and linear increase in A_{340}. This absorption is caused by the formation of a species with a λ_{max} at 340 nm that is spectrophotometrically indistinguishable from NADH. The rate of increase in A_{340} is also linearly dependent on the aldehyde concentration, and in the absence of aldehyde no specific increase in A_{340} is observed (data not shown). It is important to note that neither blank I nor blank II reactions are observed in the absence of amine-containing buffers. Incubation of acetaldehyde in sodium pyrophosphate or CAPS buffer at the same pH and temperature gives a blank rate that is <1% that observed in the presence of Tris or glycine buffers. Therefore, it is the reaction of acetaldehyde with the amine-containing buffer that is responsible for these effects.

Unmasking the True Progress Curve of NADH Formation. In order to understand the effects of these blank reactions, we have attempted to reproduce the results reported in the literature. Figure 4 shows a typical progress curve showing the change in A_{340} for the standard assay of D-ADH-dependent aldehyde oxidation in glycine buffer using the reported assay conditions (Moxon et al., 1985; Eisses, 1989).

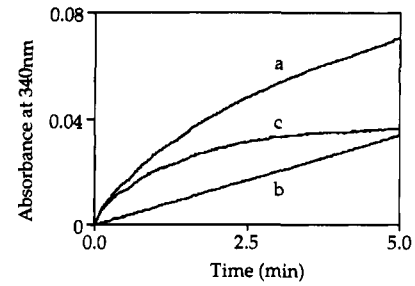

FIGURE 4: The observed spectrophotometric assay progress curve at 340 nm (a) for a mixture containing 2.0 mM NAD^+, 15.0 mM acetaldehyde, and 0.14 milliunit (mU) of D-ADH in 0.1 M glycine buffer at pH 9.5 and 30 °C, and the blank rate (b) in the same assay mixture but *without* D-ADH. Both assays were initiated by aldehyde addition. The enzymatic reaction progress curve (c) was obtained by subtraction of the nonenzymic blank reaction from the assay progress curve

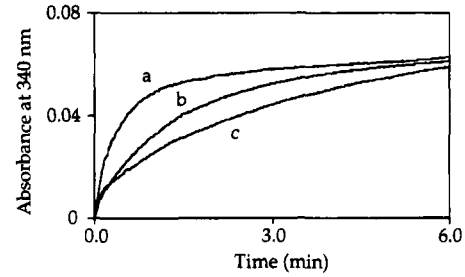

FIGURE 5: The burst of NADH formation at 340 nm as a function of enzyme concentration. Assays were carried out at 30 °C in 0.1 M CAPS buffer, pH 10, containing 2.0 mM NAD^+ and 15 mM acetaldehyde in the presence of the following amounts of D-ADH: (a) 0.14 mU; (b) 0.28 mU; (c) 0.60 mU. Assays were initiated by aldehyde addition.

A relatively rapid initial rate of increase in A_{340} is observed, followed by a slower, approximately linear steady-state increase (with incubations greater than 10 min, a more rapid, nonlinear increase begins to be observed). Obtaining reproducible data from these curves is difficult because of the curvature of the initial phase. Nonetheless, we have been able to reproduce, to within 20%, the kinetic values reported previously (Moxon et al., 1985; Eisses, 1989). As shown in Figure 4, when the blank reaction is measured under identical assay conditions (only lacking the enzyme) and is subtracted from the progress curve of the enzyme-catalyzed reaction, a very different picture emerges. Here we see that in reality the enzyme-catalyzed component of the assay progress curve is a burst of NADH formation that rapidly comes to a halt with little further D-ADH-dependent increase in A_{340} being observed. When the reaction is conducted in sodium pyrophosphate buffer, where the interfering blank reaction is negligible, the burst is readily observable without having to subtract any blank reactions (see Figure 5). Although the initial rate of NADH production *is* enzyme-dependent, the final concentration of NADH generated (magnitude of the burst) is independent of the amount of D-ADH used in the assay, as shown in Figure 5. A crucial point is that the amount of NADH generated during this burst is small, with a final concentration that is <10 μM, and represents approximately 0.5% the amount of aldehyde dismutated in the same time period (see below).

Dependence of the Burst of NADH Formation on pH. Assay progress curves have been obtained for a series of pH values in CAPS or pyrophosphate. As shown in Figure 6, we observe that the magnitude of the burst is strongly

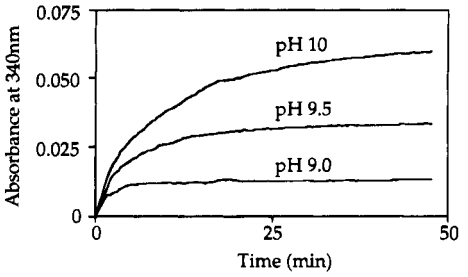

FIGURE 6: The spectrophotometric assay burst of NADH formation as a function of pH. The assay mixture at 30 °C contained 2.0 mM NAD^+, 15.0 mM acetaldehyde, and 0.12 unit of D-ADH in (a) 0.1 M CAPS buffer, pH 10.0; (b) 0.1 M sodium pyrophosphate, pH 9.5; and (c) 0.1 M sodium pyrophsphate buffer, pH 9.0. The reaction in 0.1 M sodium phosphate, pH 7.5, shows no detectable increase in A_{340} (curve not shown).

pH-dependent, becoming smaller with decreasing pH. At pH values below 9.0 no burst is detectable; i.e., the amplitude of the burst at 340 nm becomes <0.002. The diminution of the magnitude of the burst with decreasing pH is clearly the basis for previous observations that D-ADH does not exhibit aldehyde dehydrogenase activity at physiological pH of 7.5 (Benner et al., 1985; Brooks et al., 1985). Like those previous studies, we were unable to demonstrate any detectable increase in A_{340} at pH 7.5 even after prolonged incubation with high concentrations of D-ADH. Analysis of the initial rate of increase of A_{340} in assays initiated by aldehyde addition with pyrophosphate buffer at high pH yields comparable kinetic values to those reported for assays in glycine or Tris buffer at the corresponding pH. That is, the reaction between the amine buffer and acetaldehyde under these conditions does not appear to interfere with the kinetics of the initial phase of the assay. This result is consistent with the observation that the resonances of the aldehyde hydrate, the putative substrate for aldehyde oxidation, are not immediately altered by the amine buffer.

Spectrophotometric and ^1H NMR Assay of Aldehyde Oxidation. In order to understand the origins of the burst, we have measured the time-dependent changes in the composition of all the components of the assay mixture using an ^1H NMR assay based on the method previously reported from this laboratory (Henehan & Oppenheimer, 1993). As outlined in the experimental section, the time-dependent change in the concentration of the components was determined from the integrated area of their resonances which are well-resolved at 500 MHz. As a control, the total area of the methyl resonances (from 2.5 to 0.5 ppm) was integrated and found to be unchanged to within 5% over the course of the experiment. A portion of a series of ^1H NMR spectra is displayed as a stacked plot in Figure 7 and shows the time-dependent changes in the resonances for an assay mixture containing 15 mM acetaldehyde, 2.0 mM NAD^+, and 0.2 unit of D-ADH in 0.1 M sodium pyrophosphate buffer, pH 9.5. As can be seen, the disappearance of acetaldehyde occurs with a concomitant appearance of resonances due to ethanol and acetic acid which increase to millimolar concentrations; i.e., acetaldehyde is being dismutated.

In order to correlate the results for NADH production with the aldehyde dismutation reaction, parallel experiments were conducted by dividing an assay mixture into two portions; one portion was monitored spectrophotometrically while the other was followed by the ^1H NMR assay method. These

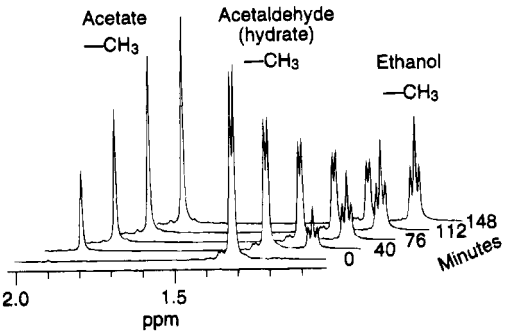

FIGURE 7: Stacked plot of a portion of the ^1H NMR spectra showing the time-dependent changes in an assay of acetaldehyde oxidation by D-ADH. The assay was carried out in 0.1 M sodium pyrophosphate buffer, pH 9.5 at 30 °C, in a final volume of 0.5 mL. Initial concentrations of assay components were NAD^+, 2.0 mM, and acetaldehyde, 15.0 mM. The reaction was initiated by addition of 0.12 unit of D-ADH.

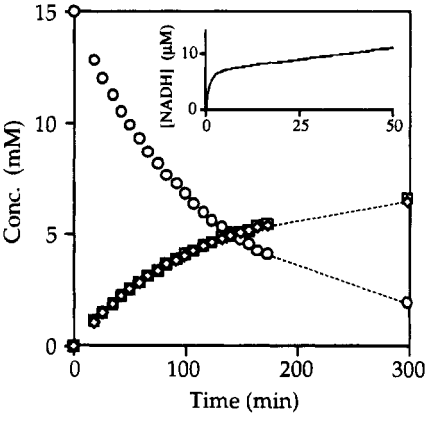

FIGURE 8: Plot of the time-dependent change in concentrations of the reaction components for the oxidation of acetaldehyde by D-ADH at 30 °C in 0.1 M sodium pyrophosphate buffer, pH 9.5. The changing concentrations of acetaldehyde (○), acetate (□), and ethanol (◇) were followed by ^1H NMR. Initial assay concentrations were NAD^+, 2.0 mM, and acetaldehyde, 15.0 mM, and the reaction was started by addition of 0.15 unit of D-ADH. The insert shows the corresponding spectrophotometric assay progress curve at 340 nm for the oxidation of acetaldehyde by D-ADH at pH 9.5 (note the thousandfold difference in scale for the concentration in the two plots).

assays contained 0.15 unit of D-ADH, 15 mM acetaldehyde, and 2.0 mM NAD^+ in 0.1 M sodium pyrophosphate buffer at pH 9.5, or in 0.1 M sodium phosphate buffer at pH 7.5. Figure 8 shows the progress curves for the D-ADH-catalyzed acetaldehyde dismutation as determined from their ^1H NMR spectra at pH 9.5, and the corresponding spectrophotometric assay progress curve is shown as an insert. As can be readily observed, in the same period of time that a 7 μM burst of NADH is produced, dismutation has produced millimolar concentrations of ethanol and acetate. Moreover, dismutation continues unabated even after there is no further rapid change in NADH concentration. Analysis of the ^1H NMR spectra establishes the initial rate of acetate and ethanol formation to be over 20 times the initial rate of NADH formation. We note that, in assays with especially high concentrations of D-ADH, after the initial burst in A_{340} a slow increase in the concentration of NADH is observed (see Figure 8 insert). The rate of this increase is about 2% the rate of the initial burst, and the subsequent increase in NADH concentration is ca. 0.2% of the change occurring in the concentration of the substrate.

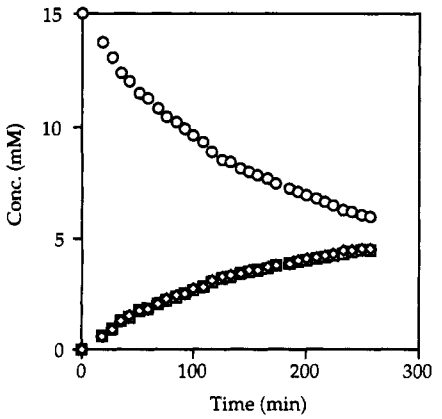

FIGURE 9: Plot of the time-dependent change in concentrations of the reaction components for the oxidation of acetaldehyde by D-ADH at 30 °C in 0.1 M sodium phosphate buffer, pH 7.5. The changing concentrations of acetaldehyde (○), acetate (□), and ethanol (◇) were followed by ^{1}H NMR. Initial assay concentrations were NAD^+, 2.0 mM, and acetaldehyde, 15.0 mM, and the reaction was started by addition of 0.15 unit of D-ADH. The corresponding spectrophotometric assay progress curve at 340 nm showed no change in absorbance at this pH (data not shown).

At pH 7.5, the spectrophotometric assay shows no change in A_{340} even after prolonged incubation (data not shown). In contrast, the ^{1}H NMR spectra of the same assay mixture (Figure 9) reveal that acetaldehyde is undergoing rapid dismutation to ethanol and acetate at a rate that is still 40% the rate of dismutation observed at pH 9.5. Therefore, D-ADH is fully capable of oxidizing aldehydes at neutral pH, and the dismutation reaction has only a modest pH dependence.

DISCUSSION

As these studies have shown, a variety of artifacts, both chemical and kinetic in nature, have prevented an accurate assessment of the ability of the *Drosophila* alcohol dehydrogenase to oxidize aldehydes. Early attempts at measuring aldehyde oxidation activity of D-ADH encountered difficulties with spectrophotometric assays, which in view of our results are understandable. These problems were initially circumvented by coupling NADH production to the reduction of a tetrazolium dye (Heinstra et al., 1983). This method was criticized (Moxon et al., 1985) because of the instability of the dye at the high pH values used and the nonphysiological concentrations of acetaldehyde (100 mM) employed for the assay. Subsequent studies adopted a spectrophotometric assay procedure based on the direct monitoring of NADH production at 340 nm in a reaction mixture containing glycine or Tris buffer at pH values ranging from 9.5 to 10.0 (Moxon et al., 1985; Eisses, 1989). The underlying limitations of this assay and the nonlinearity of the blank reaction were not discussed.

Blank Reactions. As we have shown, the reaction between the primary amino group of glycine and acetaldehyde is the source of the nonlinear blank I reaction. The magnitude of the blank I reaction has a critical dependence on the concentration of the aldehyde and the duration of the preincubation of aldehyde with the reactive buffer prior to measurement.

The second blank reaction, blank II, results from the formation of an NAD adduct of the kind described by Everse et al. (1973) (Everse et al., 1973; Arnold & Kaplan, 1974; Arnold et al., 1979). A similar adduct reaction has also been reported for aldose reductase, a member of the aldo−keto reductase superfamily (Grimshaw et al., 1990). Adduct formation has two main consequences. First, it decreases the effective coenzyme concentration in the assay; this will be especially critical at low concentrations of NAD^+. Second, 4-substituted-1,4-dihydropyridine adducts can be selective and powerful inhibitors for many dehydrogenases (Kaplan et al., 1974). This prospect is especially troublesome because it means that the assay can contain variable amounts of a potential inhibitor whose concentration will be a function of the duration of any preincubation prior to initiation of the reaction. Furthermore, during the course of the enzyme assay this reaction will generate ever higher concentrations of the adduct to where it can exceed the concentration of the NADH being generated in the burst (see Figure 4).

We note that the NAD^+ adduct being generated in glycine buffer may not be identical to that generated by the hydroxide-catalyzed reaction as described by Everse et al. (Everse et al., 1971, 1973; Arnold & Kaplan, 1974; Arnold et al., 1979). The rate of formation of the adduct is over 100 times faster in glycine and Tris buffers than in pyrophosphate buffer at the same pH. The origins of this catalysis is not obvious. If it involves addition of the Schiff base to the 4-position of the nicotinamide ring, then the resulting product could be distinct from that generated by the hydroxide-catalyzed addition and cyclization observed for carbonyls at high pH (Everse et al., 1971, 1973). We are currently investigating this reaction and its products. In any case, formation of NAD adducts is only a significant problem in solutions containing aldehydes and amine buffers at pH values above 9.

Another blank reaction known to occur is the reaction of aldehydes with the adenine base of NAD^+ (e.g., formaldehyde). For some dehydrogenases the resulting modified adenine is well tolerated, while for others this modification leads to much higher K_d values for nucleotides (see Kochetkov and Budovskii, 1972).

Summary of Blank Reactions. These experiments establish the unsuitability of buffers containing primary amine functional groups in assays to monitor aldehyde oxidation by dehydrogenases, or for that matter, reactions catalyzed by any other enzyme that utilizes aldehydes or aldoses as substrates. Quite apart from any inconvenience caused by the blank reactions, the underlying chemistry lowers the effective aldehyde and coenzyme concentrations, generates multiple components of unknown, and potentially inhibitory, properties, and prevents accurate measurement of kinetic constants by obscuring the true nature of the reaction progress curves, e.g., the burst. The nonlinearity of blank I either alone or coupled with the effects of blank II could account for the conflicting kinetic data for aldehyde oxidation by D-ADH that are reported in the literature (Moxon et al., 1985; Eisses, 1989).

It is important to note that amine-containing buffers at high pH continue to be used in assays of aldehyde oxidation (Ito et al., 1994) and aldehyde reduction (Burdette & Zeikus, 1994). We note that interference from Tris in kinetic studies of aldehyde reduction by *Pseudomonas putida* ADH has been observed, but attributed to a specific interaction with the enzyme and not to reaction of Tris with the substrate (Shaw et al., 1993).

Scheme 1

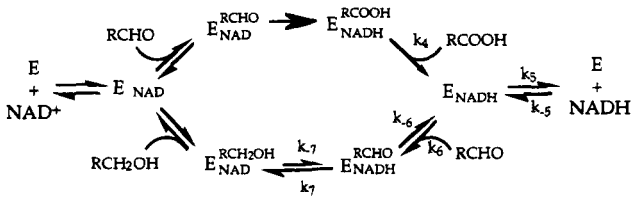

Aldehyde Dismutation Catalyzed by D-ADH. The possibility that D-ADH-catalyzed aldehyde oxidation is due to contamination by an aldehyde dehydrogenase needs to be addressed. Early studies of HL-ADH by Abeles and Lee (1960) established that the ability of that enzyme to oxidize aldehydes was an intrinsic property of the ADH and was not due to contamination with an aldehyde dehydrogenase (see also Anderson & Dahlquist, 1982). This possibility can certainly be dismissed for D-ADH because our studies have been conducted using a recombinant enzyme expressed in *Escherichia coli* which will not be contaminated by a *Drosophila* aldehyde dehydrogenase.

We conclude that the ability of D-ADH to catalyze the rapid dismutation of aldehydes is an intrinsic property of the enzyme. This finding has two important consequences. First, the kinetic values for acetaldehyde oxidation must be comparable to those for ethanol oxidation. Second, these results support the findings of Heinstra et al. (1989) that aldehyde oxidation by D-ADH can occur at physiological pH—thus the discrepancy between the *in vivo* and *in vitro* results is resolved.

Kinetic Mechanism of Aldehyde Dismutation. Scheme 1 shows the kinetic mechanism of aldehyde dismutation proposed here for D-ADH at pH 7.5 and pH 9.5. The mechanism is consistent with existing knowledge of D-ADH kinetics (Winberg & McKinley-McKee, 1988). As demonstrated in Scheme 1, the dismutation of aldehyde substrates consists of two coupled half-reactions. In the first reaction (upper pathway), aldehyde is oxidized irreversibly to the carboxylic acid and in the process forms E·NADH. In the second half-reaction (lower pathway), another molecule of aldehyde binds to the E·NADH complex and is reduced reversibly to the alcohol. The combination of the two half-reactions produces a cycle that provides for the overall dismutation of aldehydes. As long as binding of aldehyde to E·NADH (governed by k_6), and its subsequent reduction to E·NAD^+·alcohol, is fast relative to the dissociation of E·NADH (k_5), then no accumulation of NADH in the assay medium will be expected and the reaction will be redox silent; i.e., there will be no observable change in A_{340}.

Note that K_m and V_{max} for dismutation cannot be simply compared to values for either aldehyde reduction or ethanol oxidation. Obviously, the K_m for oxidation of an aldehyde cannot be measured in the normal assay (reaction 1) because of dismutation. Moreover, the K_m for aldehyde reduction is not comparable to the K_m for the reductive half-reaction of the dismutation cycle because the K_m for aldehyde reduction contains fundamental rate constants for coenzyme dissociation whereas dismutation involves no coenzyme release.

Origins of the Burst of NADH Production. Although bursts are normal in pre-steady-state kinetics, the observation of bursts in steady-state assays is much less common. There are three primary phenomenon invoked to explain the observation of a burst in steady-state assay progress curves: (1) equilibration of the reaction, (2) severe product inhibition, and (3) slow inactivation of the enzyme. None of these possibilities pertain to the burst observed for the D-ADH-catalyzed oxidation of acetaldehyde at high pH. Clearly, the burst cannot be due to equilibration of the reactants and products because oxidation of an aldehyde to a carboxylic acid is irreversible under these conditions. Product inhibition can also be ruled out because dismutation continues after the burst is over, as shown by the NMR data in Figure 8. Inhibition by an NAD−aldehyde adduct can also be ignored because the magnitude of the burst remains the same when the reaction is conducted in pyrophosphate buffer where no adduct formation is observed. Finally, no loss in enzyme activity is noted even after prolonged incubation of D-ADH with aldehydes. Therefore, the burst progress curve for D-ADH oxidation of acetaldehyde at high pH represents a novel phenomenon in steady-state kinetics and one not previously observed for any other dehydrogenase-catalyzed reaction, with the exception of the oxidation of the aldehyde, glyoxalate, by lactate dehydrogenase (Duncan, 1980).

Why does the same underlying dismutation reaction give rise to a burst of NADH formation at pH 9.5, but not at pH 7.5? These questions can be addressed by focusing on that portion of the dismutation reaction shown in Scheme 1 that involves E·NADH formation. The E·NADH complex formed by the irreversible oxidation of acetaldehyde has two fates: it can either dissociate to yield free NADH and enzyme (k_5), or it can combine with a molecule of aldehyde to form the productive E·NADH·aldehyde (k_6) complex, leading to the reduction of aldehyde to alcohol via k_7. At pH 7.5, E·NADH reacts rapidly with a molecule of aldehyde before it can dissociate to E + NADH. As a consequence, the concentration of E·NADH is low, and no detectable NADH is released into the assay medium. The same explanation has been proposed for the dismutation of acetaldehyde by HL-ADH (Dalziel & Dickinson, 1965).

At pH 9.5 we know from the NMR data that the overall reaction is still a stoichiometric dismutation of acetaldehyde except now it is accompanied by a small burst of NADH. Increasing the pH from 7.5 to 9.5 substantially decreases the rate of aldehyde reduction, whereas the rate of E·NADH dissociation (k_5 × [E·NADH]) remains unchanged (Winberg &McKinley-McKee, 1988). Therefore, E·NADH partitions between oxidation by a molecule of acetaldehyde and dissociation to NADH and free enzyme. Coenzyme dissociation gives rise to an increasing absorption at 340 nm until a steady state is reached, when the recombination of enzyme and NADH to give E·NADH (governed by k_{-5} × [NADH][E]) becomes equal to k_5 x [E·NADH]; i.e., the E·NADH complex has come to equilibrium with enzyme and NADH. When NADH reaches its equilibrium concentration, the burst plateaus and the rate of aldehyde oxidation to the carboxylic acid becomes equal to the rate of aldehyde reduction to alcohol. The slow drift in NADH concentrations seen after the burst is due to the alcohol product of the reaction, which will cause a slow increase in E·NADH (and therefore free NADH) with time due to reversal of the steps of alcohol production.

This model explains why the magnitude of the burst is independent of enzyme concentration (as shown in Figure 5); an increase in enzyme concentration will produce an increase in the rate of formation of E·NADH but also an equal increase in the rate of reduction of aldehyde by

E·NADH. Overall, the concentration of E·NADH remains unchanged. We note that the burst behavior of D-ADH is strikingly similar to that reported for the disproportionation of glyoxalate catalyzed by rabbit muscle lactate dehydrogenase (Duncan, 1980), and we suggest that the behavior of both enzymes has similar origins.

An important point is that the initial rate of increase of A_{340} measured at high pH is not a direct function of the actual rate of aldehyde oxidation. Therefore, any kinetic constants determined using this assay are invalid as a measure of the rate of aldehyde oxidation. They cannot be used to draw conclusions about the metabolic function of D-ADH *in vivo*, nor can they be compared to those for other dehydrogenases, or to the activity of D-ADH with alcohols.

Alcohol Dehydrogenases Mimicking Aldehyde Dehydrogenases. The ability of an ADH to oxidize/dismutate aldehydes can be manifest in three distinct ways when monitored by changes in A_{340}. Previously, we have shown for HL-ADH that if dismutation is fast, and continues in the presence of high concentrations of alcohol and acid, a lag will be observed in A_{340} progress curve (Henehan & Oppenheimer, 1993). Alternatively, when aldehyde traps E·NADH generated by aldehyde oxidation and reoxidizes it back to E·NAD$^+$ before it can dissociate, then dismutation will occur without generation of detectable NADH, e.g., as observed for D-ADH at neutral pH. Finally, if E·NADH can partition between its oxidation by aldehydes and dissociation of NADH, then NADH will build up to detectable concentrations, manifest as a burst in A_{340}, e.g., as observed for D-ADH at high pH. It follows that some of the reported aldehyde dehydrogenases in the literature could be alcohol dehydrogenases "masquerading" as aldehyde dehydrogenases. For example, Ito et al. (1994) have reported the isolation of a formaldehyde dehydrogenase from *P. putida*. However, this enzyme is structurally related to the medium chain alcohol dehydrogenases, it is assayed with formaldehyde as substrate in glycine buffer, and the reaction is monitored at 340 nm. This enzyme has all the hallmarks of an alcohol dehydrogenase exhibiting NADH formation as part of a dismutation reaction.

Mechanistic Implications of Aldehyde Oxidation by ADHs. HL-ADH and D-ADH are broad spectrum alcohol dehydrogenases that are physically, mechanistically, evolutionarily, and stereochemically distinct (Persson et al., 1991). Both catalyze the oxidation of primary and secondary alcohols, and as we have demonstrated, they also conduct the facile oxidation of aldehydes to carboxylates. This, taken together with the observation that lactate dehydrogenase can catalyze the oxidation of glyoxalate (Duncan, 1980), establishes that members of all three major families of alcohol dehydrogenases are multifunctional enzymes, capable of catalyzing the oxidation of alcohols to aldehydes as well as aldehydes to carboxylates. Given the fundamental structural and mechanistic differences between the three families, we conclude that the ability to conduct both alcohol and aldehyde oxidations must be an intrinsic and fundamental property of the dehydrogenation reaction itself and not of the specific mechanism by which catalysis is achieved.

These results demonstrate that the distinctions between what is considered to be an alcohol dehydrogenase and an aldehyde dehydrogenase are blurred and that all the catalytic activities of alcohol dehydrogenases must be evaluated as part of their kinetic characterization and in order to elucidate their physiological function.

REFERENCES

Abeles, R. H., & Lee, H. A. (1960) *J. Biol. Chem. 235*, 1499–1503.

Anderson, D. C., & Dahlquist, F. W. (1982) *Arch. Biochem. Biophys. 217*, 226–235.

Arnold, L. J., Jr., & Kaplan, N. O. (1974) *J. Biol. Chem. 149*, 652.

Arnold, L. J., Jr., Oppenheimer, N. J., Lee, C.-Y., & Kaplan, N. O. (1979) *Biochemistry 18*, 2787–2793.

Benner, S. A., Nambiar, K. P., & Chambers, G. K. (1985) *J. Am. Chem. Soc. 107*, 5513–5517.

Brooks, W. M., Moxon, L. N., Field, J., Irving, M. G., & Doddrell, D. M. (1985) *Biochem. Biophys. Res. Commun. 128*, 107–112.

Burdette, D., & Zeikus, J. G. (1994) *Biochem. J. 302*, 163–170.

Chen, Z., Shirley, M., Lee, W. R., & Chang, S. H. (1990) *Biochemistry 29*, 1112–1118.

Dalziel, K., & Dickinson, F. M. (1965) *Nature 206*, 255–257.

Dickinson, F. M., & Monger, G. P. (1973) *Biochem. J. 131*, 261–270.

Duncan, R. J. S. (1980) *Arch. Biochem. Biophys. 201*, 128–136.

Eisses, K. T. (1989) *Bioorg. Chem. 17*, 268–274.

Everse, J., Zoll, E. P., & Kahan, L. (1971) *Bioorg. Chem. 1*, 207–233.

Everse, J., Zoll, E. C., Kahan, L., & Kaplan, N. O. (1973) *Adv. Enzymol. 37*, 61–133.

Glasoe, P. K., & Long, F. A. (1960) *J. Chem. Phys. 64*, 188–190.

Grimshaw, C. E., Shabbaz, M., & Putney, C. G. (1990) *Biochemistry 29*, 9936–9946.

Heinstra, W. H., Eisses, K. T., Schoonen, W. G. E. J., Aben, W., Winter, A. J. d., Horst, D. J. v. d., Marrewijk, W. J. A. v., Beenakkers, A. M. T., Scharloo, W., & Thorig, G. E. W. (1983) *Genetica 60*, 129–137.

Heinstra, P. W. H., Geer, B. W., Seykens, D., & Langevin, M. (1989) *Biochem. J. 259*, 791–797.

Henehan, G. T. M., & Oppenheimer, N. J. (1993) *Biochemistry 32*, 735–738.

Henehan, G. T. M., Kenyon, G. L., & Oppenheimer, N. J. (1993) in *Enzymology and Molecular Biology of Carbonyl Metabolism 4* (Weiner, H., Crabbe, D. W., & Flynn, T. G., Eds.) pp 481–491, Plenum Press, New York and London.

Hinson, J. A., & Neal, R. A. (1972) *J. Biol. Chem. 247*, 7106–7107.

Hore, P. J. (1989) *Methods Enzymol. 176*, 64–77.

Ito, K., Takahashi, M., Yoshimoto, T., & Tsuru, D. (1994) *J. Bacteriol. 176*, 2483–2491.

Jörnvall, H., Eklund, H., & Branden, C. I. (1978) *J. Biol. Chem. 253*, 8414–8419.

Kaplan, N. O., Everse, J., Dixon, J. E., Stolzenbach, F. E., Lee, C.-Y., Lee, C.-L., Taylor, S. S., & Mosbach, K. (1974) *Proc. Natl. Acad. Sci. U.S.A. 71*, 3450–3454.

Kochetkov, N. K., & Budovskii, E. I. (1972) in *Organic Chemistry of Nucleic Acids*, pp 355–375, Plenum Press, New York.

Moxon, L. N., Holmes, R. S., Parsons, P. A., Irving, M. G., & Doddrell., D. M. (1985) *Comp. Biochem. Physiol. 80B (3)*, 525–535.

Oppenheimer, N. J., & Handlon, A. L. (1992) *Enzymes 20*, 454–505.

Oppenheimer, N. J., & Henehan, G. T. M. (1995) in *Enzymology and Molecular Biology of Carbonyl Metabolism 5* (Weiner, H., Holmes, R. S., & Wermuth, B., Eds.) pp 407–415, Plenum Press, New York and London.

Persson, B., Krook, M., & Jörnvall, H. (1991) *Eur. J. Biochem. 200*, 537–543.

Shaw, J. P., Rekik, M., Schwager, F., & Harayama, S. (1993) *J. Biol. Chem. 268*, 10842–10847.

Tsai, C. S., & Sher, D. S. (1980) *Arch. Biochem. Biophys. 199*, 626–634.

Winberg, J.-O., & McKinley-McKee, J. S. (1988) *Biochem. J. 255*, 589–599.

BI950861Y